

# Practical Policy Distillation for Reinforcement Learning in Radio Access Networks

Sara Khosravi, Burak Demirel, Linghui Zhou, Javier Rasines, Pablo Soldati

Ericsson AB, Kista, Sweden

email:{name.surname}@ericsson.com

**Abstract**—Adopting artificial intelligence (AI) in radio access networks (RANs) presents several challenges, limited availability of link-level measurements (e.g., CQI reports), stringent real-time processing constraints (e.g., sub-1 ms per TTI), and network heterogeneity (different spectrum bands, cell types, and vendor equipment). A critical yet often overlooked barrier lies in the computational and memory limitations of RAN baseband hardware—particularly in legacy 4<sup>th</sup> Generation (4G) systems—which typically lack on-chip neural accelerators. As a result, only lightweight AI models (under 1 Mb and sub-100  $\mu$ s inference time) can be effectively deployed, limiting both their performance and applicability. However, achieving strong generalization across diverse network conditions often requires large-scale models with substantial resource demands. To address this trade-off, this paper investigates *policy distillation* in the context of a reinforcement learning-based link adaptation task. We explore two strategies: *single-policy distillation*, where a scenario-agnostic teacher model is compressed into one generalized student model; and *multi-policy distillation*, where multiple scenario-specific teachers are consolidated into a single generalist student. Experimental evaluations in a high-fidelity, 5<sup>th</sup> Generation (5G)-compliant simulator demonstrate that both strategies produce compact student models that preserve the teachers’ generalization capabilities while complying with the computational and memory limitations of existing RAN hardware.

**Index Terms**—Artificial intelligence, reinforcement learning, policy distillation, radio access networks.

## I. INTRODUCTION

Artificial intelligence (AI) is increasingly recognized as a key enabler of improved performance and efficiency in radio access networks (RANs). AI-driven solutions have been explored across a broad range of RAN functions, including channel estimation and symbol decoding at the physical layer [1], [2]; fast control loops, such as link adaptation and

radio resource management, at the medium access layer [3]–[6]; and slower functionalities such as mobility management, load balancing, and network configuration [7], [8]. Factors such as user mobility, interference, traffic fluctuations, and the heterogeneity of both RAN infrastructure and user equipment (UE) introduce significant variability. As a result, achieving reliable performance in real-world RAN deployments requires AI models that can adapt to diverse and dynamic network conditions [9]. In other words, models must generalize effectively and perform robustly, even on previously unseen data [10].

Training an AI model for a RAN function to generalize across diverse RAN environments—rather than fine-tuning separate models for specific conditions, such as those encountered in a single radio cell—is essential for scalable AI integration in RANs [9]. Reducing model proliferation enables more efficient and cost-effective lifecycle management. In contrast, models fine-tuned to specific network conditions often lack the robustness required to adapt to changes in network and environmental dynamics, necessitating frequent updates and compromising performance consistency. However, achieving effective model generalization requires extensive and diverse training data, as well as sufficiently large models capable of learning and extrapolating complex patterns from large datasets [10].

Although RANs are data-rich systems, a fundamental challenge in deploying AI within existing infrastructure is the computational constraint of legacy baseband hardware. Designed primarily for efficient signal processing and protocol execution, 4<sup>th</sup> Generation (4G) and 5<sup>th</sup> Generation (5G) baseband units were not dimensioned to support large AI models. As a result, a mismatch often arises between the demands of AI-based network optimization and the limited hardware resources available for inference in RAN systems. This restricts the size and complexity of models that can be practically deployed, thereby limiting their ability to generalize effectively.

Knowledge distillation [11] has been proposed to address the challenge of deploying complex models on resource-constrained devices. It enables knowledge transfer from a large, high-performing teacher model to a smaller, computationally efficient student model, with negligible degradation in accuracy [12]. Originally introduced for supervised learning tasks [12], [13], recent work [14], [15] has extended these techniques to *policy distillation* in reinforcement learning for control applications. However, the ability of policy distillation to retain the generalization capability of the teacher model—and

© 2025 IEEE. Personal use of this material is permitted. Permission from IEEE must be obtained for all other uses, in any current or future media, including reprinting/republishing this material for advertising or promotional purposes, creating new collective works, for resale or redistribution to servers or lists, or reuse of any copyrighted component of this work in other works.

This is the author’s version of the paper accepted for publication in *IEEE International Symposium on Personal, Indoor and Mobile Radio Communications*, 2025. The final published version is available at IEEE Xplore, <https://doi.org/10.1109/PIMRC62392.2025.11274591>.

its applicability to practical problems in RANs—remains relatively unexplored.

This paper explores policy distillation as a method to replace traditional RAN functions with AI-based alternatives under realistic RAN operational constraints. Our goal is to distill AI models that comply with RAN baseband hardware constraints while retaining the sophisticated decision-making capabilities of large, computationally intensive teacher models. Focusing on the link adaptation (LA) function, we employ *domain randomization* to generate diverse training datasets from varied simulated environments. These datasets are then used to train compact, computationally efficient student models that closely replicate the behavior of high-capacity teacher models. We evaluate two distillation strategies: *single-policy* distillation, which compresses a single scenario-agnostic teacher into a compact student model; and *multi-policy* distillation, which integrates knowledge from multiple scenario-specific teachers into a generalist student model. Experimental evaluations in a 5G-compliant simulator confirm both strategies dramatically reduce model size while preserving strong generalization.

## II. THE HIDDEN CHALLENGES OF AI IN RAN

Significant research has been devoted to AI-driven solutions for various RAN functions, examining algorithms, models, training methods, and data collection strategies. However, limited attention has been paid to the *real-time processing constraints* that hinder the deployment of AI in practical RAN settings. Existing RAN baseband hardware—typically based on FPGA, ASIC, or DSP architectures optimized for specialized, repetitive signal processing tasks (e.g., FFT, modulation/demodulation) and protocol execution—was not originally designed to support AI workloads, such as tensor computations or floating-point operations. Consequently, current hardware lacks the flexibility and computational headroom (e.g., memory and processing resources) required to effectively support large AI models. Additionally, baseband units commonly operate at full computational capacity under strict latency and power constraints, necessitating minimal—ideally zero—additional overhead from any AI integration.

Another crucial constraint is the stringent latency requirement of critical user-plane functions in Layer 1 (L1) and Layer 2 (L2), such as resource scheduling and link adaptation. These functions must execute within tens of microseconds—for example, link adaptation (LA) typically requires less than ten microseconds—thereby significantly limiting permissible inference latency. These latency constraints restrict AI model complexity, memory footprint, and per-inference computational cost, often limiting feasible AI models to sizes no larger than a few tens of kilobytes due to limited on-chip memory and strict inference-time budgets. Collectively, these constraints underscore the need for efficient AI deployment strategies tailored specifically to legacy RAN infrastructure.

To address these challenges, we investigate policy distillation—a technique that transfers knowledge from large, computationally intensive AI models to smaller models suitable for resource-constrained hardware. We apply this approach to

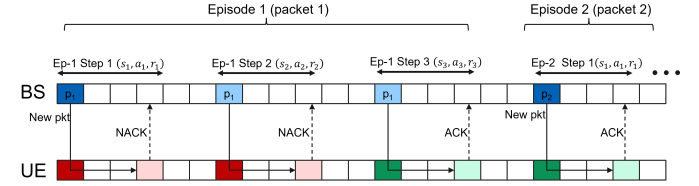


Fig. 1: Example of MDP episode definition for LA.

LA, an L2-critical-loop RAN function executed multiple times (once per scheduled UE) on a sub-millisecond timescale.

## III. PROBLEM FORMULATION

We consider the problem of LA in the downlink of a RAN, where the transmission rate is dynamically adjusted to match the link capacity by optimizing the modulation and coding scheme (MCS) parameters based on time- and frequency-varying channel conditions and radio interference. In 5G systems, the MCS parameters—comprising the modulation order and code rate—are represented by an MCS index [16], denoted by integer values  $m$  ranging from 0 to  $M - 1$ .

LA algorithms deployed in present-day RANs typically rely on two control loops: an inner loop that maps the latest channel state information (CSI) reported by a UE to an initial signal-to-interference-plus-noise ratio (SINR) estimate, and an outer loop that adjusts this estimate based on hybrid automatic repeat request (HARQ) feedback to maximize spectral efficiency while meeting a target block error rate (BLER). However, the outer loop converges slowly [17] to a fixed BLER target; therefore, it struggles to adapt to dynamic channel conditions under bursty traffic. In contrast, reinforcement learning (RL)-based approach can learn a policy that predicts the optimal MCS index in real time, offering the potential to overcome the limitations of rule-based LA algorithms.

### A. RL-based Link Adaptation

We model the LA problem as an episodic Markov decision process (MDP)  $\mathcal{M} = \langle \mathcal{S}, \mathcal{A}, \mathcal{P}, \mathcal{R}, \gamma \rangle$ , where each episode corresponds to the lifespan of a UE data packet—from its first transmission to either successful reception or packet drop after  $N$  transmission attempts, as illustrated in Fig. 1. The action space  $\mathcal{A} = \{a \mid a \in \{0, \dots, M - 1\}\}$  comprises  $M$  discrete values, representing the MCS indices used to adapt the link spectral efficiency. In our evaluations, we consider 28 MCS indices (i.e.,  $M = 28$ ), as defined in Table 5.1.3.1-2 of the 5G specifications [16].

Following [18], we use a reward function  $r_n = r(s_n, a_n) \in \mathcal{R}$  for each individual packet transmission, defined as

$$r_n = \begin{cases} SE_n, & \text{if successfully received at } n^{\text{th}} \text{ TX,} \\ -\alpha \cdot n, & \text{if unsuccessfully received at } n^{\text{th}} \text{ TX,} \end{cases} \quad (1)$$

where  $n \in \{0, \dots, N - 1\}$  is the packet transmission index,  $\alpha \in \mathbb{R}_+$  is a penalty coefficient for retransmissions, and  $SE_n$  denotes the spectral efficiency achieved upon successful reception in the  $n^{\text{th}}$  transmission attempt.

To support model generalization across the RAN environment during training, we consider two key enablers. First, we design the state  $s \in \mathcal{S}$  to encapsulate a mixture of semi-static and dynamic information. The semi-static information serves two purposes: (i) to characterize the heterogeneity of the RAN deployment and its configuration relative to the UE—including deployment type, location, orientation, inter-relations among network sites or radio cells, and parameters such as antenna array type, carrier frequency, bandwidth, and transmit power—and (ii) to describe the UE’s characteristics (e.g., chipset and capabilities), enabling the model to operate across a diverse set of devices. The dynamic information, in contrast, captures state variables relevant to LA behavior, such as path loss, CSI, HARQ feedback, and many more; see, e.g., [18] for the complete list of states.

Additionally, we leverage a distributed training architecture combined with domain randomization to improve model robustness by exposing the agent to varied and diverse environmental conditions. Domain randomization introduces controlled stochasticity into the training environment to bridge the simulation-to-reality gap, as further described in Section V.

#### IV. POLICY DISTILLATION

To address the challenge of achieving model generalization while adhering to the constraints imposed by RAN hardware, we merge knowledge distillation with domain randomization.

Knowledge distillation, referred to as *policy distillation* in the RL context [14], involves transferring a policy learned by an agent (the teacher), through interaction with an environment, into a smaller, simpler model (the student) without significant performance degradation. Policy distillation can be performed in both online and offline settings [14], [15], [19]. In *online policy distillation*, the student model learns concurrently with the teacher, as the latter improves its policy through ongoing interaction with the environment. In contrast, *offline policy distillation* assumes that the teacher has been fully trained. The student is then trained using a dataset generated by the teacher’s fixed policy.

In this paper, we only focus on the offline approach, assuming a trained deep Q-network (DQN) policy for LA as the teacher, following the design presented in Section III.

##### A. Offline Policy Distillation

Following [19], we consider a distillation dataset  $\mathcal{D}^T = \{(s_i, \mathbf{q}_i^T)\}_i$ , where each sample  $i$  consists of a state  $s_i \in \mathcal{S}$  from the LA function and a vector of unnormalized Q-values  $\mathbf{q}_i^T = \pi^T(s_i)$  produced by the teacher policy  $\pi^T$ . These Q-values serve as target outputs for training a student policy  $\pi^S$ .

To guide the training, we employ the Kullback-Leibler (KL) divergence loss, defined as

$$L_{\text{KL}}(\mathcal{D}^T, \pi^S) = \sum_{i=1}^{|\mathcal{D}^T|} \text{softmax}\left(\frac{\mathbf{q}_i^T}{\tau}\right) \ln \frac{\text{softmax}(\frac{\mathbf{q}_i^T}{\tau})}{\text{softmax}(\mathbf{q}_i^S)}. \quad (2)$$

Here, a softmax transformation is applied to both the teacher’s Q-values  $\mathbf{q}_i^T$ , scaled by a temperature parameter  $\tau > 0$ , and the

student’s Q-values  $\mathbf{q}_i^S$ , which are left unscaled. In the context of policy distillation, Rusu *et al.* [19] recommend using lower values of  $\tau$  to sharpen the output distribution. Since Q-values represent the expected future discounted rewards for each possible action, sharpening accentuates the differences in action preferences and improves the fidelity of the transferred policy.

Unlike prior work, our objective is to distill a student policy  $\pi^S$  that retains the teacher’s generalization capability while being significantly more compact. To this end, we revisit and extend two offline policy distillation strategies: single- and multi-policy distillation [19].

##### B. Generalization via Single-Policy Distillation

Our first approach combines single-policy distillation with domain randomization. In this case, we distill a student policy  $\pi^S$  from the knowledge of a single expert-level teacher  $\pi^T$ . However, to retain the teacher’s ability to generalize across the RAN environment, the distillation dataset  $\mathcal{D}^T$  must capture the teacher’s behavior under diverse radio communication conditions. To this end, we also apply domain randomization when generating the distillation samples  $(s_i, \mathbf{q}_i^T)$ , as described in Section V, ensuring that the state samples  $s_i$  are drawn from heterogeneous network deployments with varying configurations, radio environments, traffic and interference types, load conditions, user device types, and so on.

Practical RAN deployments are, by nature, a source of extreme diversity due to the variety of radio environments, network configurations, traffic patterns, and interference distributions encountered across radio cells. Therefore, if a teacher model is trained using the collective experience of distributed actors operating in different radio cells, a diverse distillation dataset  $\mathcal{D}^T$  can be constructed by reusing data stored in the teacher’s replay memory. Specifically, the trained teacher can be evaluated on state observations  $s_i$  already present in the replay memory used during training.

##### C. Generalization via Multi-Policy Distillation

Our second approach is inspired by multi-policy distillation. Training a large RL teacher model from the collective experience of radio cells across a live RAN can be costly and may negatively impact RAN performance due to the exploration process. As an alternative path to achieving model generalization under hardware constraints, we propose training multiple teacher models using less invasive methods and applying multi-policy distillation to induce generalization by fusing their policies into a single student model.

Specifically, we consider  $N$  independently trained teacher policies  $\pi^{T_j}$ , each specialized—rather than generalized—for a specific network environment or deployment. This allows each teacher model to be dimensioned according to the hardware constraints of the target RAN. For instance, different teacher models may be trained separately using drive tests in specific network contexts (e.g., urban, rural, high-speed), as well as with proprietary networks, lab testbeds, or high-fidelity network simulators.

After training a set of teacher models, we generate the corresponding distillation datasets, denoted as  $\mathcal{D}^{T_j} = \{(s_i, \mathbf{q}_i^{T_j})\}_{i=0}^{D_j}$  for all  $j \in \{0, \dots, N-1\}$ , following the same methodology as in single-policy distillation. We then shuffle and aggregate these datasets to train a unified student model. Since the student learns from the combined behavior of multiple specialized teachers, the resulting policy generalizes effectively across diverse RAN environments.

## V. NUMERICAL EXAMPLES

To evaluate the potential of knowledge distillation for facilitating the deployment of AI in RANs, we focus on its ability to reduce model size to meet the hardware limitations of current RAN technology while achieving the performance and retaining the generalization capability of a larger teacher model. To this end, we consider both single-policy and multi-policy distillation applied to a RL policy for MCS index selection in downlink LA, and compare the performance of a larger teacher model against multiple student models of varying size across a range of performance metrics. To assess whether the student models retain the generalization ability of the teacher, we evaluate them using three representative benchmark scenarios not encountered during training. Furthermore, we demonstrate that training a small model directly with RL—rather than applying policy distillation—fails to achieve comparable performance and generalization.

### A. Training Setup

To train the teacher models, similar to [18], we use a large-scale distributed training architecture, in which a single learner updates the model using the collective experience of multiple distributed actors and broadcasts the updated model parameters to the actors. Each actor interacts with several parallel simulations based on a 5G-compliant event-driven network simulator. Each training simulation emulates a time-division duplex system operating at a 3.5 GHz carrier frequency, with physical layer numerology  $\mu = 0$ , and single-user multiple input multiple output (SU-MIMO) transmission according to a parameter configuration sampled from Table I. However, we adopt a different training approach for teachers used in single-policy and multi-policy distillation, as discussed later.

For both single- and multi-policy distillation, we employ a teacher architecture consisting of a 7-layer multi-layer perceptron (MLP) with 128 neurons per layer ( $7 \times 128$ ), comprising approximately 105 k parameters. We distill three student models of different sizes: (i) a 4-layer MLP with 64 neurons per layer ( $4 \times 64$ ); (ii) a 4-layer MLP with 32 neurons per layer ( $4 \times 32$ ); and (iii) a 3-layer MLP with 32 neurons per layer ( $3 \times 32$ ). These correspond to approximately 15 k, 5 k, and 3.5 k model parameters, respectively.

### B. Testing Setup

To assess model generalization, we evaluate all models against three benchmark scenarios not explicitly encountered during training: single-cell single-user (SCSU), multiple input

Parameter	Value range
Antenna array	$1 \times 2 \times 2$ MIMO (4) $8 \times 4 \times 2$ mMIMO (64)
Cell radius	{166, 300, 600, 900, 1200} m
Bandwidth	{20, 40, 50, 80, 100} MHz
Number of sub-bands	{51, 106, 133, 217, 273}
DL TX power	{20, 40, 50, 80, 100} W
UE antennas	{2, 4}
Maximum TX rank	{2, 4}
Maximum DL TX	5
Number FB UEs	{1, 5, 10}
Number MBB UEs	{5, 10, 25, 50, 100, 150}
Speed UE FB	{0.67, 10, 15, 30} m/s
Speed UE MBB	{0.67, 1.5, 3} m/s
Indoor probability	{0.2, 0.4, 0.8}

TABLE I: Parameters for domain randomization.

multiple output (MIMO), and massive MIMO (mMIMO), each assuming three cells with full buffer (FB) traffic and 10 UEs.

We begin by evaluating the teacher model against the LA baseline commonly adopted in present-day RANs, as described in Section IV. In our benchmark scenarios, the teacher achieves an average UE throughput gain of 12% and a spectral efficiency (SE) improvement of 8% over the baseline, demonstrating its ability to perform well in diverse scenarios not seen during training. However, since our primary objective is to assess whether policy distillation can retain the teacher's generalization capability while significantly reducing model size, we focus our analysis on comparing student performance with that of the corresponding teacher across the three benchmark scenarios.

We consider three performance metrics: average UE throughput ( $T$ ), BLER, and episodic reward ( $r$ ). The results are reported using the *relative gain/loss*. Values close to zero indicate that the student models closely approximate the teacher's behavior. For example, the relative throughput gain/loss ( $\Delta T$ ) is computed as:

$$\Delta T = 100 \times \frac{T_{\text{student}} - T_{\text{teacher}}}{T_{\text{teacher}}}.$$

Analogous definitions apply to  $\Delta \text{BLER}$  and  $\Delta r$ . Finally, to assess whether the distillation process effectively transfers the teacher's policy, we compare the probability density function (PDF) of the actions returned by the teacher and the corresponding student models in each benchmark scenario.

### C. Generalization via Single-Policy Distillation

We apply single-policy distillation to an RL policy for MCS index selection in downlink LA, trained to generalize across the RAN environment. To this end, we combine the previously introduced distributed RL training architecture with domain randomization to improve model resilience to uncertainties in the RAN environment, such as network deployment and configuration, traffic conditions, and user population.

Specifically, we train the teacher model using 5000 simulations, distributed across 16 actors, each with randomized network parameters based on Table I. Each simulation lasts

Distillation	Student Model	MIMO Scenario			mMIMO Scenario			SCSU Scenario		
		$\Delta T$	$\Delta \text{BLER}$	$\Delta r$	$\Delta T$	$\Delta \text{BLER}$	$\Delta r$	$\Delta T$	$\Delta \text{BLER}$	$\Delta r$
Single-policy	Student $4 \times 64$	+0.04%	+4.7%	-0.5%	-0.02%	+2.4%	-0.8%	-0.21%	+2.1%	-0.8%
	Student $4 \times 32$	+0.14%	+2.3%	-0.9%	+0.15%	0.0%	-1.2%	+0.02%	-6.6%	-1.1%
	Student $3 \times 32$	-0.17%	+6.5%	-1.7%	+0.09%	+4.7%	-1.7%	-0.54%	+6.5%	-2.2%
Multi-policy	Student $4 \times 64$	-1.2%	+4.8%	-2.5%	-1.0%	-2.7%	-0.8%	-1.6%	+2.5%	-0.8%
	Student $4 \times 32$	-2.3%	+2.9%	-3.3%	-1.9%	-3.7%	-1.2%	-1.9%	-2.5%	-1.6%
	Student $3 \times 32$	-2.8%	+5.7%	-3.7%	-2.3%	-4.0%	-1.5%	-2.2%	0.0%	-1.9%

TABLE II: Relative gain/loss (%) of student models with respect to their teacher models, across performance metrics and benchmark scenarios.

3 seconds and consists of one to three tri-sectorial radio sites, randomly configured as MIMO or mMIMO, according to antenna characteristics in Table I. Site parameters such as inter-site distance, cell radius, bandwidth, and downlink transmit power are also randomly sampled from Table I. Further randomization includes cell loads, traffic types, indoor/outdoor UE ratios, and UE receiver types. UEs are generated with random counts of FB and mobile broadband (MBB) traffic, with traffic patterns modeled from real-world data. UE configurations—including the number of antenna elements, speed, and receiver type—are randomized to reflect hardware and algorithmic differences across devices (e.g., CSI estimation).

To enable the distillation process to retain the generalization capability of the teacher model, we further apply domain randomization to generate the distillation dataset  $\mathcal{D}^T$  by testing the teacher against 1000 randomized network simulations, resulting in approximately 20 million samples—providing sufficient data diversity for effective distillation.

Figure 2 and Table II (single-policy rows) demonstrate that distilling a teacher model (7 layers of 128 units) into progressively smaller student models—from 4 layers of 64 units down to 3 layers of 32 units, representing approximately a 30-fold compression—can effectively preserve performance. Specifically, throughput degradation remains within 1% across the MIMO, mMIMO, and SCSU scenarios; BLER deviation is limited to within  $\pm 7\%$  relative to the teacher model, with the mid-sized student model (4 layers of 32 units) even achieving a 6.6% improvement in BLER for SCSU. Moreover, the episodic reward declines by no more than 1.7%. In contrast, the control model (3 layers of 32 units), trained from scratch, significantly underperforms—by approximately 12% in MIMO, 10% in mMIMO, and 25% in SCSU—as indicated by the purple markers falling clearly below the 0% reference line in Fig. 2.

Figure 3 further confirms that the distilled student models effectively replicate the teacher model’s behavior, both in terms of throughput and the actions selected. Specifically, Fig. 3(a)–(c) illustrate a near-perfect overlap between the teacher (blue) and student models (orange, green, red) in the cumulative distribution function (CDF) of UE throughput. In contrast, the smaller control model trained from scratch (purple) deviates considerably—especially in the SCSU scenario. Similarly, Fig. 3(d)–(f) confirm that the student models closely match the teacher’s distribution of MCS indices. The control model, however, collapses onto a limited subset of indices, displaying pronounced peaks near indices 10 and 16, and

rarely selecting indices above 19.

Collectively, these results confirm that single-policy distillation, when combined with domain randomization, effectively preserves the teacher model’s generalization capability, even after substantial compression—approximately 30-fold. Directly training a similarly sized model, however, leads to poor generalization performance.

#### D. Generalization via Multi-Policy Distillation

Table II (multi-policy rows) shows that a single student model, distilled from the combined knowledge of three scenario-specific teacher models, closely retains the performance of the original experts despite an approximate 30-fold parameter reduction (to a model with 3 layers of 32 units). Across the three benchmark environments, the throughput deficit of the smallest student model never exceeds  $-2.8\%$  (MIMO scenario), while the larger student models maintain throughput within  $-1.0\%$  to  $-2.3\%$ . Changes in BLER remain modest, ranging from an improvement of  $-4.0\%$  (mMIMO scenario) to a maximum increase of  $+5.7\%$  (MIMO scenario), never exceeding a  $+6\%$  deviation. The maximum observed reduction in episodic reward is  $3.7\%$ . Collectively, these tight performance bounds indicate that multi-policy distillation effectively compresses and integrates specialized knowledge from multiple scenario-specific expert models into a single lightweight generalist model capable of robustly generalizing across diverse benchmark conditions.

## VI. CONCLUSIONS

In this paper, we demonstrated that policy distillation is a viable approach to replacing traditional RAN functions with AI-based counterparts that conform to the computational and memory constraints of existing baseband hardware. Focusing on the LA function, we applied domain randomization to assemble richly varied training sets from multiple simulated RAN scenarios. These datasets enabled us to train lightweight student models that faithfully imitate the decision logic of high-capacity teacher models. We assessed two distillation paradigms: (i) single-policy distillation, which compresses a unified, scenario-agnostic teacher into a compact student; and (ii) multi-policy distillation, which merges the expertise of several scenario-specific teachers into a single generalist student. Through experiments, we showed that both strategies substantially reduce model size—bringing their footprints well within existing hardware limits—while retaining near-teacher

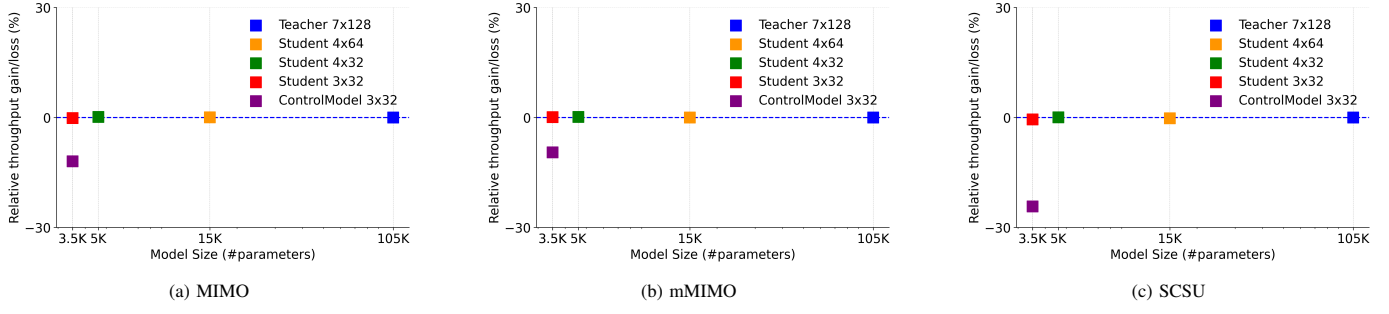


Fig. 2: Comparison of the average throughput achieved by each student relative to the teacher in the MIMO, mMIMO and SCSU benchmark scenarios.

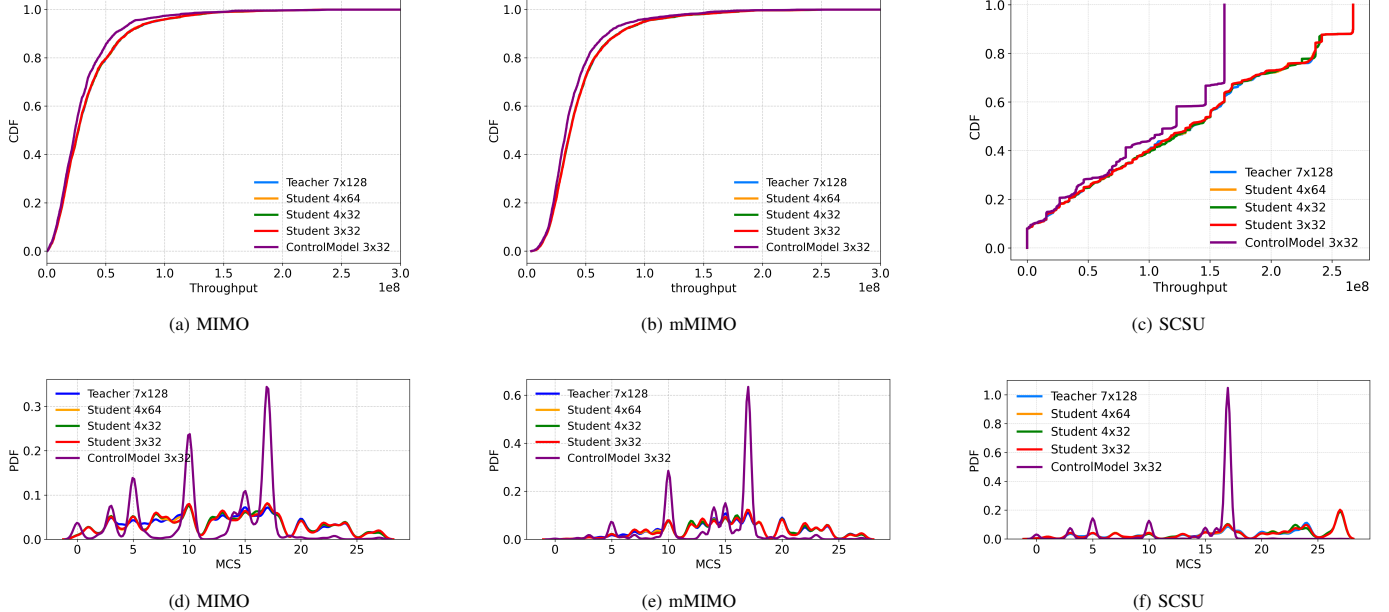


Fig. 3: Comparison of the teacher and students policies across the three benchmark scenarios in terms of: CDF of the UE throughput (a)-(c); and actions distribution, represented by the PDF of selected MCS values (d)-(f).

performance and broad generalization across diverse network conditions. Our findings underscore policy distillation as a practical, minimally invasive pathway for embedding AI-driven RAN functions into current deployments.

## REFERENCES

- [1] M. S. V. Pourahmadi, A. Mirzaei, and H. Sheikhzadeh, “Deep learning-based channel estimation,” *IEEE Communications Letters*, vol. 23, no. 4, 2019.
- [2] S. Srivastava and P. P. Dash, “ML-based reconfigurable symbol decoder: An alternative for next-generation communication systems,” *Engineering Applications of Artificial Intelligence*, vol. 114, 2022.
- [3] P. Kela, T. Höhne, T. Veijalainen, and H. Abdulrahman, “Reinforcement learning for delay sensitive uplink outer-loop link adaptation,” in *2022 Joint European Conference on Networks and Communications & 6G Summit (EuCNC/6G Summit)*, 2022.
- [4] J. Chen, J. Ma, Y. He, and G. Wu, “Deployment-friendly link adaptation in wireless local-area network based on on-line reinforcement learning,” *IEEE Communications Letters*, vol. 27, no. 12, pp. 3424–3428, 2023.
- [5] F. D. Calabrese, L. Wang, E. Ghadimi, G. Peters, L. Hanzo, and P. Soldati, “Learning radio resource management in RANs: Framework, opportunities, and challenges,” *IEEE Communications Magazine*, vol. 56, no. 9, pp. 138–145, 2018, publisher: IEEE.
- [6] D. Sandberg, T. Kvernvik, and F. D. Calabrese, “Learning robust scheduling with search and attention,” in *Proc. of the IEEE International Conference on Communications (ICC)*, 2022, pp. 1549–1555.
- [7] A. F. Ashour and M. M. Fouad, “AI-based approaches for handover optimization in 5g new radio and 6g wireless networks,” in *Proc. of the International Conference on Computer Science, Information Technology and Engineering (ICCoSITE)*, 2023, pp. 336–341.
- [8] E. Gures, I. Shaya, M. Ergen, M. H. Azmi, and A. A. El-Saleh, “Machine learning-based load balancing algorithms in future heterogeneous networks: A survey,” *IEEE Access*, vol. 10, pp. 37 689–37 717, 2022.
- [9] P. Soldati, E. Ghadimi, B. Demirel, Y. Wang, R. Gaigalas, and M. Sinton, “Design principles for model generalization and scalable AI integration in radio access networks,” *IEEE Communications Magazine*, no. 9, pp. 1–8, 2024, publisher: IEEE.
- [10] Z. Tu, F. He, and D. Tao, “Understanding Generalization in Recurrent Neural Networks,” in *International Conference on Learning Representations (ICLR)*, 2020.
- [11] J. Gou, B. Shen, F. Du, and F. Wu, “Knowledge Distillation: A Survey,” *International Journal of Computer Vision*, vol. 129, no. 6, pp. 1789–1819, 2021.
- [12] G. Hinton, O. Vinyals, and J. Dean, “Distilling the Knowledge in a Neural Network,” *arXiv preprint arXiv:1503.02531*, 2015. [Online]. Available: <https://arxiv.org/abs/1503.02531>
- [13] C. Bucilu, R. Caruana, and A. Niculescu-Mizil, “Model compression,” in *Proc. of the 12th ACM SIGKDD Intern. Conference on Knowledge Discovery and Data Mining*, 2006, p. 535–541.
- [14] A. A. Rusu, S. G. Colmenarejo, C. Gulcehre, G. Desjardins, J. Kirkpatrick, R. Pascanu, V. Mnih, K. Kavukcuoglu, and R. Hadsell, “Policy distillation,” 2016. [Online]. Available: <https://arxiv.org/abs/1511.06295>

- [15] Y. Sun and P. Fazli, "Real-time policy distillation in deep reinforcement learning," *NeurIPS*, vol. abs/1912.12630, 2019. [Online]. Available: <https://api.semanticscholar.org/CorpusID:209515823>
- [16] 3GPP, "Technical Specification (TS) 38.214. NR, NR; Physical layer procedures for data, v18.3.0," Jun. 2024.
- [17] F. Blanquez-Casado, G. Gomez, M. d. C. Aguayo-Torres, and J. T. Entrambasaguas, "eOLLA: an enhanced outer loop link adaptation for cellular networks," *EURASIP Journal on Wireless Communications and Networking*, vol. 2016, pp. 1–16, 2016, publisher: Springer.
- [18] B. Demirel, Y. Wang, C. Tatino, and P. Soldati, "Generalization in reinforcement learning for radio access networks," 2025. [Online]. Available: <https://arxiv.org/abs/2507.06602>
- [19] A. A. Rusu, S. G. Colmenarejo, C. Gulcehre, G. Desjardins, J. Kirkpatrick, R. Pascanu, V. Mnih, K. Kavukcuoglu, and R. Hadsell, "Policy distillation," *arXiv preprint arXiv:1511.06295*, 2016. [Online]. Available: <https://arxiv.org/abs/1511.06295>